Cell Surface Heparan Sulfate Proteoglycan Syndecan-2 Induces the Maturation of Dendritic Spines in Rat Hippocampal Neurons

Iryna M. Ethell and Yu Yamaguchi

The Burnham Institute, La Jolla, California 92037

Abstract. Dendritic spines are small protrusions that receive synapses, and changes in spine morphology are thought to be the structural basis for learning and memory. We demonstrate that the cell surface heparan sulfate proteoglycan syndecan-2 plays a critical role in spine development. Syndecan-2 is concentrated at the synapses, specifically on the dendritic spines of cultured hippocampal neurons, and its accumulation occurs concomitant with the morphological maturation of spines from long thin protrusions to stubby and headed shapes. Early introduction of syndecan-2 cDNA into immature hippocampal neurons, by transient transfection, accelerates spine formation from dendritic protrusions. Deletion of the COOH-terminal EFYA motif of syndecan-2, the binding site for PDZ domain proteins, abrogates the spine-promoting activity of syndecan-2. Syndecan-2 clustering on dendritic protrusions does not require the PDZ domain-binding motif, but another portion of the cytoplasmic domain which includes a protein kinase C phosphorylation site. Our results indicate that syndecan-2 plays a direct role in the development of postsynaptic specialization through its interactions with PDZ domain proteins.

Key words: syndecan-2 • heparan sulfate proteoglycan • dendritic spines • hippocampal neurons

The importance of structural elements in learning and memory has long been recognized (Hebb, 1949; Edwards, 1995; reviewed in Milner et al., 1998). Structural modifications of synapses play a critical role in regulating the plasticity underlying learning and memory (Calverley and Jones, 1990; Yuste and Denk, 1995). Dendritic spines are small protrusions on the surface of dendrites that receive the majority of excitatory synapses (Harris and Kater, 1994). Several studies have shown that morphological changes to dendritic spines occur during long-term potentiation, sensory deprivation, and the rearing of animals in enriched environments (Fifkova, 1985; Lund et al., 1991; Wallace et al., 1991; Rollenhagen and Bischof, 1994; Buchs and Muller, 1996; Comery et al., 1996; Durand et al., 1996). Abnormal spine morphologies have been shown to be associated with some forms of mental retardation and autism, including fragile X syndrome (Rudelli et al., 1985; Hinton et al., 1991; Comery et al., 1997). Elucidation of the molecular mechanism for spine development is key for understanding the mechanisms involved in learning and memory, as well as mental retardation.

Cell adhesion has been implicated in the structural modification of synapses (Lüthi et al., 1994; Spacek and Harris, 1998; reviewed in Rose, 1995; Colman, 1997; Serafini, 1997; Hagler and Goda, 1998). Among different classes of molecules involved in cell–matrix adhesion, heparan sulfate proteoglycans (HSPGs)[1] have been shown to be present in neuromuscular junctions (Eldridge et al., 1986; Cole and Halfter, 1996; Meier et al., 1998) and proposed to be key molecules of adhesion-induced synaptic modifications (Schubert, 1991). The functional relationships between classic cell adhesion molecules, like cadherins, IgCAMs, integrins, and functionally ambiguous proteoglycan-related molecules in synaptic junctions still remain to be determined.

Syndecans are a major class of cell surface HSPGs (reviewed in Bernfield et al., 1992; Couchman and Woods, 1996; Carey, 1997). Four members of the syndecan family, syndecan-1, -2, -3, and -4, have been cloned from mammalian species. The core proteins of syndecans consist of a structurally diverse extracellular domain, highly conserved transmembrane, and cytoplasmic domains. The extracellular domain carries several heparan sulfate chains, which bind a number of heparin-binding molecules, including growth factors, extracellular matrix, and cell adhesion proteins (reviewed in Couchman and Woods, 1996; Carey, 1997).

Address correspondence to Yu Yamaguchi, The Burnham Institute, 10901 North Torrey Pines Road, La Jolla, CA 92037. Tel.: 619-646-3124. Fax: 619-646-3199. E-mail: yyamaguchi@burnham-inst.org

Abbreviations used in this paper: DIV, days in vitro; E, embryonic day; GFP, green fluorescent protein; HSPG, heparan sulfate proteoglycan; PKC, protein kinase C; PSD, postsynaptic density.

Syndecans are known to be concentrated at specific sites on the cell surface (reviewed in Couchman and Woods, 1996; Carey, 1997). It has been shown that syndecan-1 colocalizes with actin filaments in areas of cell–matrix adhesion (Carey et al., 1994), syndecan-2 is expressed at sites of cell–cell and cell–matrix interactions (David et al., 1993), and syndecan-4 is localized to focal adhesions (Woods and Couchman, 1994). Mechanisms for the targeting of syndecans toward specific membrane sites are not completely understood, although phosphorylation and molecular interactions of their cytoplasmic domains are thought to play roles in these processes. The cytoplasmic domains of syndecans contain several potential phosphorylation sites. There are four tyrosine residues conserved among all members of the family, including invertebrate syndecans. In addition, syndecan-2 has a unique serine phosphorylation site for protein kinase C (PKC). It has been shown that syndecan-2 can be serine phosphorylated by Ca^{2+}-dependent or conventional isoforms of PKC α, β, and γ, and that phosphorylation is dependent on the oligomerization of its cytoplasmic domain (Itano et al., 1996; Oh et al., 1997). The cytoplasmic domain of syndecan-1 is required for its colocalization with actin filaments (Carey et al., 1994, 1996). Moreover, the COOH-terminal EFYA motif of syndecan-2, identical in all members of the syndecan's family, can interact with PDZ domain proteins, such as syntenin (Grootjans et al., 1997) and the postsynaptic protein CASK (Cohen et al., 1998; Hsueh et al., 1998). PDZ domain proteins are thought to play critical roles in the organization of postsynaptic specializations (Craven and Bredt, 1998). Thus, syndecans could provide a molecular link between intracellular cytoskeleton/signaling complex and the extracellular environment at specific sites on the cell surface.

In this paper, we present evidence indicating that syndecan-2 plays a critical role in the maturation of dendritic spines. Syndecan-2 is highly concentrated on the spines of mature hippocampal neurons in culture, and its clustering occurs concomitant with the morphological maturation of spines. Most importantly, we demonstrate that forced expression of syndecan-2 in young neurons, by transient transfection, causes early transformation of immature dendritic protrusions into morphologically mature spine-like structures. Moreover, by introducing syndecan-2 deletion mutants, we demonstrate that the interaction of syndecan-2 with PDZ domain proteins is involved in the morphological maturation of dendritic spines. However, deletion of the PDZ domain binding site of syndecan-2 did not affect the spine-specific targeting and clustering of syndecan-2, suggesting that these processes require other parts of the cytoplasmic domain, that include potential serine and tyrosine phosphorylation sites. Thus, we show a direct functional role for syndecan-2 in spine development, and suggest that the cell surface HSPG syndecan-2 is involved in molecular interactions underlying postsynaptic modifications.

Materials and Methods

RNA Purification and Reverse Transcriptase-PCR

Total RNA was extracted from cultures of rat hippocampal neurons at different time points by using Triazol reagents (Life Technologies, Inc.). Reverse transcriptase PCR (RT-PCR) was performed with 2 μg of total RNA as described previously (Watanabe and Yamaguchi, 1996) with the following primer pairs (forward and backward, respectively): syndecan-1 CCCAAGCTTGGGATGACTCTGACAACTTC and GGTATAGCATGAAAGCCACCAGACGTCAA; syndecan-2 CGGAATTCTCAACCCATCGGCTGCTTGCTT and GCTCTAGACCTTAGTGGGTGCCTTCTGGTA; syndecan-3 CCCAAGCTTAGCGAGCGAACGAACGAGCGA and CGGGATCCTGAACCGCATGGCTGTCTCAAG; syndecan-4 CGGAATTCATGAAGACGCTGGGGGCCTTGA and CGGGATCCAATCCTCAACTCCTCTCCCCATGA; glypican-1 CCCAAGCTTTCGGCTTTTGTTGTCTCCGCCTCC and CGGGATCCAAGGCCCGAGTGTTCTGCGTGTAC; glypican-2 CCCAAGCTTTGTTCAGTTTTGGGGGGGACGCT and CGGGATCCGGGAATACAGGCGACCATAGGAAT; perlecan CCCAAGCTTGGACTTTCAGATGGTTTATTTCCG and CGGGATCCCCGCTGGAAATGACTGTGTGCA; agrin CGGAATTCACTCCATAAGAACTCCCACACAC and GCTCTAGATGGCACAGGCATGACTAAGCAG. Each set of primers was designed from rat cDNA sequences. PCR products were analyzed on agarose gel and purified using Qiagen spin columns. All positive PCR products were isolated from the gel and confirmed to be the authentic fragments by sequencing.

Primary Cultures of Rat Hippocampal Neurons

Hippocampal neurons were prepared from embryonic day (E) 17–18 rat embryos and cultured according to Zafra et al. (1990) with minor modifications. Briefly, after trypsinization and mechanical dissociation, hippocampal cells suspended in DME supplemented with 10% FCS were preplated on uncoated culture plates for 2 h to remove glial cells. Neurons recovered as nonadherent cells were plated on coverslips coated with poly-DL-ornithine (0.5 mg/ml) and laminin (5 μg/ml) at densities of 5×10^4 cells per coverslip. Neurons were cultured in serum-free DME supplemented with insulin (150 mg/ml) under 5% CO_2/10% O_2 atmosphere at 37°C (Brewer and Cotman, 1989). Cultures were maintained up to 40 d.

Construction of Syndecan Deletion Mutants

Full-length and truncated rat syndecan-2 cDNAs were amplified by RT-PCR from hippocampal neuron total RNA. The following pairs of oligonucleotide primers were used. For full-length syndecan-2 cDNA: forward, 5′-CGGAATTCTCAACCCATCGGCTGCTTGCTT; reverse, 5′-CTGGGCCCGTCATGCATAAAACTCCTTAGTGGGTGC. For syndecan-2 Δcyto cDNA: forward, 5′-CGGAATTCTCAACCCATCGGCTGCTTGCTT; reverse 5′-CTGGGCCCGTCACCGCATGCGGTAC. Amplified cDNAs were ligated into EcoRI/ApaI-cut pEGFPN1 (CLONTECH Laboratories, Inc.). The syndecan-2 ΔEFYA deletion mutant was generated by mutagenizing the glutamic acid and phenylalanine residues of the full-length syndecan-2 construct into two stop codons by using QuickChange Site-Directed Mutagenesis kit (Stratagene). All constructs were confirmed by sequencing.

Transfection of Hippocampal Neurons

Transient transfection of rat hippocampal neurons was performed at 1 day in vitro (DIV) by the calcium phosphate coprecipitation method (Chen and Okayama, 1987). Briefly, 10:1 or 1:1 mixtures of various syndecan-2 expression constructs and pEGFPC1 (for green fluorescent protein, GFP, expression) were precipitated in 400 μl of calcium-containing phosphate buffer (MBS transfection kit; Stratagene) for 20 min at room temperature. DNA precipitates diluted in complete medium were added to coverslips of 1 DIV hippocampal neurons, plated at 2×10^5 per 12-mm coverslip and cells were incubated for 6 h at 35°C under 3% CO_2. The cells were washed gently three times (15 min each) with culture media, and maintained under 5% CO_2/10% O_2 at 37°C. Transfected neurons have been shown to express significant levels of GFP for 8 d after transfection.

Immunofluorescence

To localize heparan sulfate or syndecan-2 immunoreactivity in cultured rat hippocampal neurons, cells were stained alive or fixed in ice-cold methanol for 20 min at −20°C. Live staining was carried out at room temperature in DME containing 10% FCS. Cells were incubated for 1 h with one of the following primary antibodies: anti–heparan sulfate mAb 10E4 (JgM; 1:50 dilution; Seikagaku America, Inc.) or anti–syndecan-2 polyclonal antibody (pAb) #903 (1:100 dilution; gift from Dr. Merton Bern-

field). Fluorescein-conjugated goat anti–mouse IgM (1:50 dilution; Cappel Laboratories) or rhodamine-conjugated anti–rabbit IgG (1:100 dilution; Chemicon International, Inc.) was used for immunofluorescent staining of heparan sulfate or syndecan-2, respectively. Then cells were processed for double immunolabeling by fixation in 4% paraformaldehyde in PBS for 0.5 h at room temperature and blocking in 5% normal goat serum (NGS) for 1 h. After permeabilization in 0.2% Triton X-100/PBS for 10 min, cells were washed with PBS containing 0.2% Tween 20 and 1% NGS and incubated with the following primary antibodies diluted in the washing solution: anti-NCAM pAb (IgG; 1:100; gift from Dr. Vladimir Berezin), anti-MAP2 mAb (IgG; 1:100; Sigma Chemical Co.); anti–synapsin I pAb (IgG; 1:100; gift from Dr. Andrew Czernik), and antisynaptophysin mAb (IgG; 1:100; Sigma Chemical Co.). Incubation with primary antibodies was performed at room temperature for 2 h. Bound antibodies were detected with rhodamine-conjugated goat anti–mouse IgG (1:50 dilution; Cappel Laboratories), or rhodamine-conjugated anti–rabbit IgG (1:100 dilution; Chemicon International), or fluorescein-conjugated anti–mouse IgG (1:100 dilution; Chemicon International).

For double immunostaining with anti-postsynaptic density (PSD) 95 mAb (JgG; 1:100; clone 6G6, Affinity Bioreagents) and anti–heparan sulfate or anti–syndecan-2 antibodies, cells were fixed in methanol for 20 min at −20°C and further processed as described in Kornau et al. (1995).

For immunostaining of transfected hippocampal neurons with anti–syndecan-2 pAb neurons at 8 DIV were fixed in 4% paraformaldehyde in PBS for 0.5 h at room temperature, preblocked, and incubated with primary antibodies as described above. Bound antibodies were detected with rhodamine-conjugated secondary antibody. The cells were mounted using fluorescence H-1000 medium (Vector Labs) and analyzed by confocal microscopy.

Confocal Imaging

Immunofluorescent staining was analyzed using Zeiss LSM-410 and Bio-Rad MRC 1024 confocal laser scanning microscopes. Optical sections of the hippocampal neurons were taken at an interval of 0.3 μm in the X-Y plane. To make different experiments comparable, all pictures were taken under the same parameters. The maximal intensity three-dimensional images are the results of projection of the optical serial sections. For double immunofluorescent staining, identical section series were selected.

For the analysis of dendritic protrusions/spines, transiently transfected GFP-positive or DiO-injected hippocampal neurons were analyzed using an oil immersion, 100 × 1.4 NA objective. In the case of syndecan-2/GFP double transfection, only those neurons that were immunopositive for syndecan-2 or its deletion mutants were considered as syndecan-2 transfected or syndecan-2 ΔEFYA transfected, correspondingly. Neurons that were positive for GFP, but did not express syndecan-2 were considered as control transfected. Serial optical sections were taken at an interval of 0.2 μm for each image with 4× zoom. For quantitative analysis, the numbers of protrusions/spines were counted in the proximal 50-μm segments of dendrites. Hidden spines that protrude toward the back or front of the viewing plane were not counted. Length of protrusions/spines was determined using MetaMorph software by measuring distance between its tip and base. In each experiment, at least 200 spines were counted from >10 neurons. Statistical analyses was performed using Microsoft Excel. Groups of spines were compared with Student's *t* test.

For analysis of dendritic spine morphology in nontransfected cultures, 1–4 wk after plating cultures were fixed in 4% paraformaldehyde in PBS for 30 min, individual cells were microinjected with FAST DiO (D-3898; Molecular Probes, Inc.). Coverslips were placed at 4°C in 2% paraformaldehyde in PBS for an additional 24 h to allow dye to transport before confocal microscopy. Confocal microscopy was performed as described above.

Results

Localization of Heparan Sulfate in Hippocampal Neurons

Heparan sulfate immunoreactivity has been found previously in adult rat hippocampus (Goedert et al., 1996; Fuxe et al., 1997). To define the precise localization of heparan sulfate on neuronal cell surfaces, we used glia-free monolayer cultures of E 17–18 rat hippocampal neurons. In these cultures, neurons form synapses and establish neuronal circuits in the course of 3–4 wk in vitro. Immunofluorescent staining for heparan sulfate was performed on these neurons at different stages in culture with the 10E4 mAb that recognizes intact heparan sulfate chains (David et al., 1992; Goedert et al., 1996). The expression of heparan sulfate is weak and diffuse during the first 2 wk in culture (Fig. 1, A and B), but then increases during the following weeks. At 3 wk in vitro, heparan sulfate immunoreactivity was detectable as punctate signals distributed on the cell bodies and dendrites (Fig. 1 C). The punctate staining became even stronger at 4 wk in vitro (Fig. 1, D and F). This timing of heparan sulfate expression temporally coincided with the widespread formation of dendritic spines (Fig. 1, E–H). At 1 wk in vitro, when the majority of dendritic protrusions were long, thin filopodia (Fig. 1 G), heparan sulfate immunostaining was very weak and did not show any distinct pattern of distribution (Fig. 1 E). By 4 wk in vitro, the majority of postsynaptic sites developed into stubby or mushroom-shaped mature spines (Fig. 1 H), morphologically similar to the spines seen in vivo. At the same time, strong heparan sulfate immunoreactivity was detected as puncta along the dendrites (Fig. 1 F). These re-

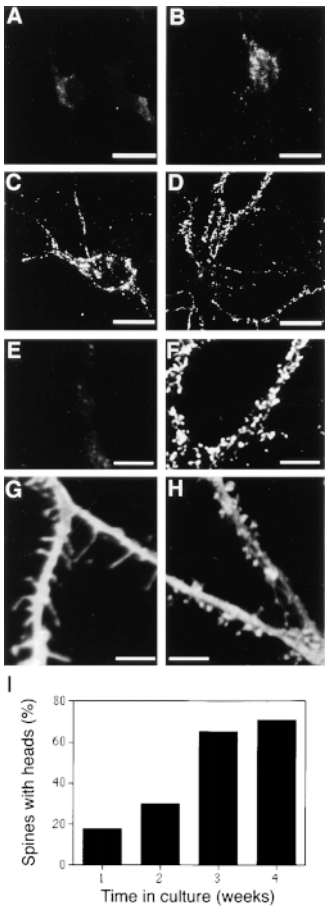

Figure 1. Time course of heparan sulfate expression and maturation of dendritic spines in hippocampal neurons at 1–4 wk in vitro. Hippocampal neurons were stained with 10E4 anti–heparan sulfate mAb at 1 (A), 2 (B), 3 (C), and 4 (D) wk in culture. Punctate pattern of heparan sulfate immunoreactivity became detectable on the surfaces of cell bodies and dendrites at 3 wk in vitro. (E and F) High-power image of heparan sulfate immunoreactivity along dendrites at 1 and 4 wk in vitro, correspondingly. (G and H) Confocal images of proximal dendrites in DiO-injected hippocampal neurons at 1 (G) and 4 (H) wk in culture. The dendritic protrusions at 1 wk in vitro are long, thin filopodia without heads (G). At 4 wk the majority of dendritic protrusions have mature mushroom shapes with thin necks and large heads (H). Bars, 20 μm in A–D and 3 μm in E–H. (I) Formation of mature spines with thin neck and a distinct head over the course of 1–4 wk in culture. Percentage of spines with heads was counted in 1-, 2-, 3-, and 4-wk-cultures. A more than twofold increase in number of headed spines was seen between 2 and 3 wk in culture.

sults suggested that heparan sulfate may be associated with dendritic spines.

To localize cell surface heparan sulfate immunoreactivity on hippocampal neurons at 30 DIV, cells were first stained alive for heparan sulfate, with subsequent fixation and double immunostaining for synapsin I, a specific marker of presynaptic boutons. Confocal microscopy revealed close apposition of cell surface heparan sulfate and synapsin I immunoreactivities (Fig. 2, A–E). Frequently they showed partial, but not complete, overlap (Fig. 2, B and C). This staining pattern suggests that cell surface heparan sulfate is associated with the synaptic junctions of cultured hippocampal neurons. Double labeling of methanol-fixed 30 DIV hippocampal neurons with antibodies to heparan sulfate and PSD-95 further confirmed the synaptic localization of heparan sulfate. Punctate immunoreactivities of heparan sulfate and PSD-95 colocalized well on dendrites (Fig. 2, F–I). There was some nonoverlapping immunostaining for heparan sulfate in perikaryon and proximal dendrites. This staining was not seen in the case of immunolabeling of live cells (Fig. 2 D), suggesting that some heparan sulfates are associated with intracellular compartments. Double staining for heparan sulfate and either MAP2, a dendritic marker (Fig. 3, A–E), or NCAM (Fig. 3, F–H) further demonstrated a punctate distribution of cell surface heparan sulfate along the dendrites of hippocampal neurons. High-power confocal imaging revealed the localization of heparan sulfate on small protrusions on the shafts of dendrites (Fig. 3, D, E, and H). These results strongly suggest that heparan sulfate is present in dendritic spines. Interestingly, while pyramidal neurons, which comprise the majority of cells in these cultures, had these heparan sulfate-immunoreactive protrusions, we occasionally found neurons that were positive for MAP2 but negative for heparan sulfate (arrows in Fig. 3, A–C). These neurons had smaller cell bodies and more satellite shapes than pyramidal neurons, a morphology consistent with that of local interneurons, that were present in these cultures as a minor population. It has been shown that local interneurons tend to lack dendritic spines (Harris and Kater, 1994). Taken together, these results demonstrate localization of cell surface heparan sulfate to the dendritic spines of hippocampal pyramidal neurons.

Temporal Expression of Different Heparan Sulfate Proteoglycans in Cultured Hippocampal Neurons

To identify the molecular species of HSPGs expressed in the dendritic spines, we performed RT-PCR analysis. Pairs of specific oligonucleotides were designed for eight different HSPGs known to be expressed in nervous tissues. Among the HSPGs examined, no expression of perlecan, agrin, or syndecan-3 was detected at any stage of

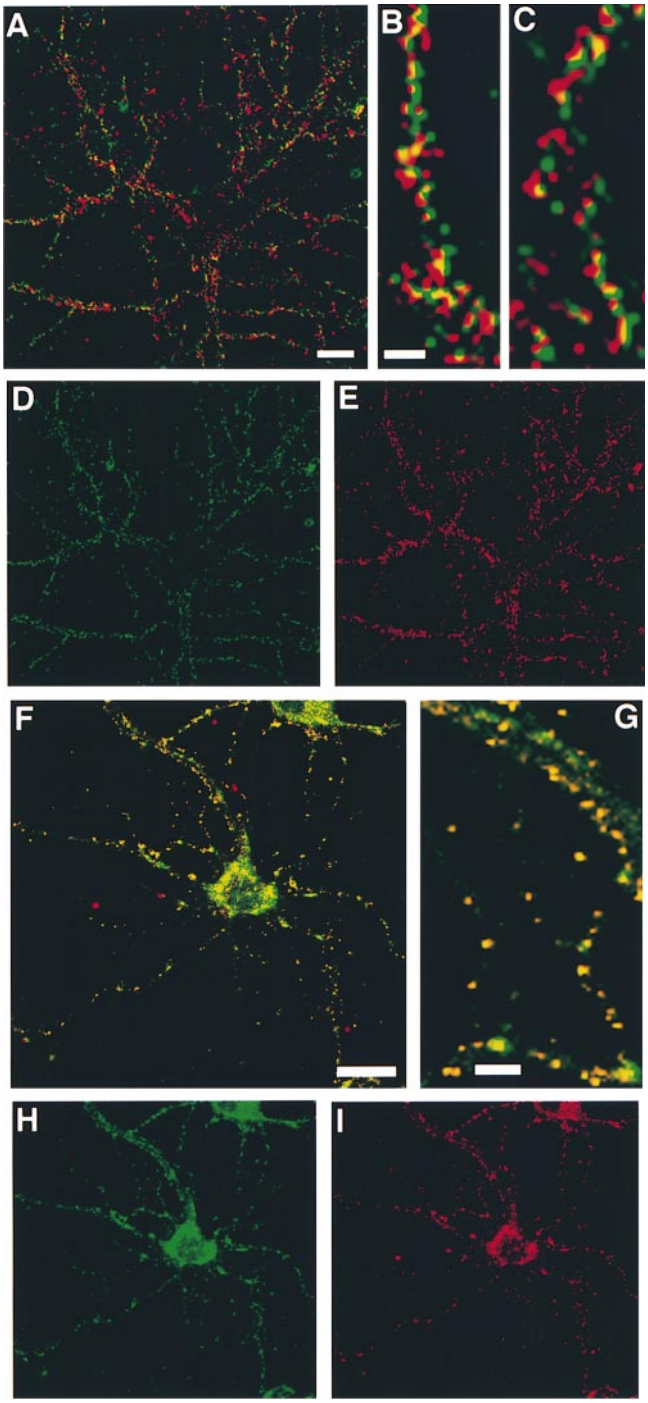

Figure 2. Postsynaptic localization of heparan sulfate in primary cultures of rat hippocampal neurons. (A–E) Confocal images of double immunolabeling of hippocampal neurons at 30 DIV for cell surface heparan sulfate 10E4 (D, green) and presynaptic marker, synapsin I (E, red). Cell surface heparan sulfate immunoreactivity (green) shows a punctate pattern on the surface of dendrites similar to synapsin I–positive staining. (B and C) High-power view reveals close apposition with only partial overlap (yellow) of immunoreactivities for synapsin I (red) and cell surface heparan sulfate (green), suggestive of synaptic localization of heparan sulfate. Bars, 20 μm in A and 10 μm in B and C. (F–I) Double immunolabeling with anti–heparan sulfate (green) and anti–PSD-95 (red) antibodies in methanol-permeabilized 30 DIV rat hippocampal neurons. Punctate immunoreactivity for heparan sulfate (green) was colocalized with PSD-95 (red) mostly on dendrites and partially cell bodies (yellow in F). (G) High-power view shows colocalization of heparan sulfate (green) and PSD-95 (red) in yellow. Some nonoverlapping immunostaining for heparan sulfate is seen in perikaryon and proximal dendrites due to intracellular heparan sulfate immunoreactivity, and was not seen in the case of alive cell surface immunolabeling (D, see Materials and Methods). Bars, 20 μm in F and 10 μm in G.

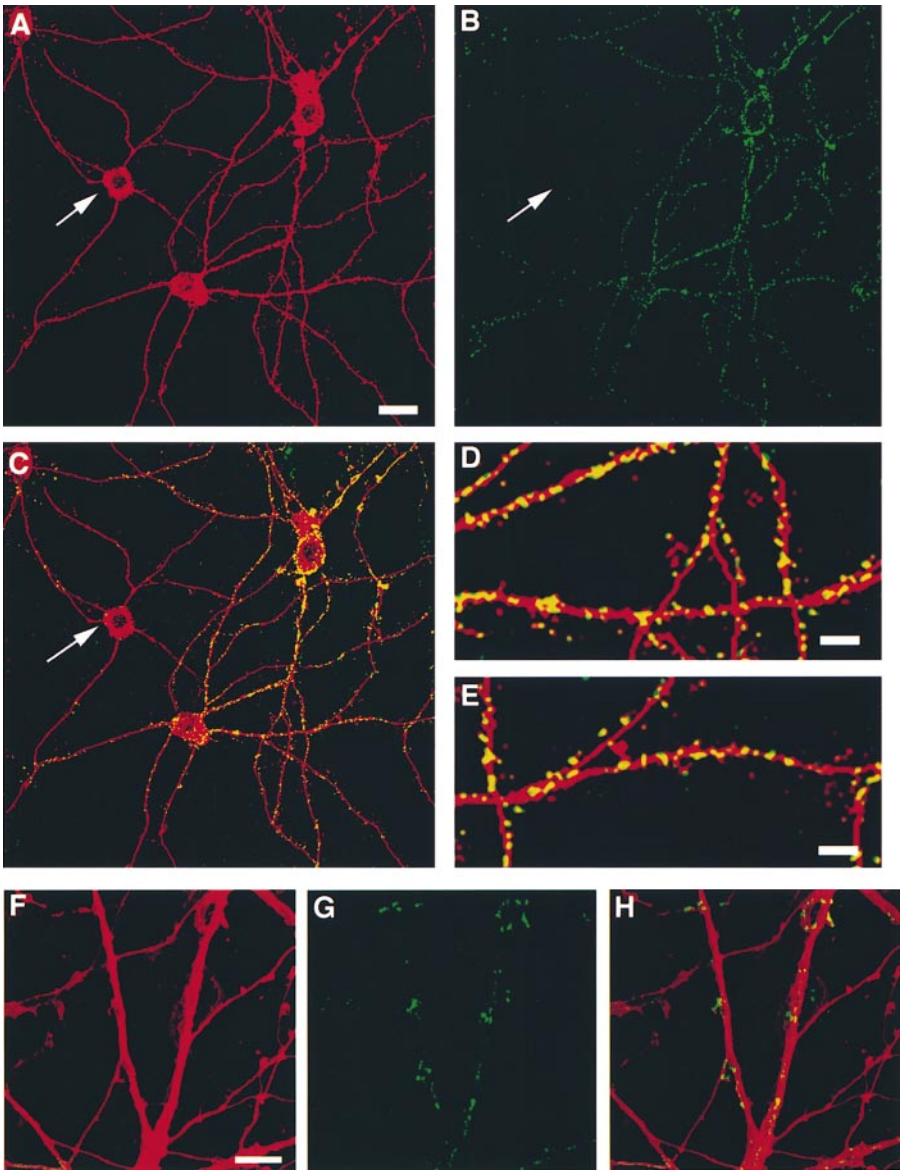

Figure 3. The expression of heparan sulfate on dendritic spines of cultured hippocampal neurons. (A–E) Double immunostaining of hippocampal neurons at 30 DIV with anti-MAP2 (red) and the 10E4 anti–heparan sulfate (green) antibodies. Cell surface heparan sulfate immunoreactivity is detected on the cell bodies and along dendrites of the pyramidal neurons. Interneurons occasionally present in these cultures are not stained for heparan sulfate (arrows). (D and E) High-power confocal image shows cell surface heparan sulfate immunoreactivity (yellow) as a puncta on the surface of MAP2-positive dendrites (red), in patterns and shapes reminiscent of dendritic spines. Bar, 20 μm in A and 10 μm in D and E. (F–H) Double immunostaining of 30 DIV hippocampal neurons with anti-NCAM (red) and anti–heparan sulfate 10E4 (green) antibodies. Heparan sulfate immunoreactivity is detected on dendritic spines, which appear as small protrusions on dendritic shafts. Bar, 10 μm.

culture (not shown). Syndecan-1, glypican-1, and glypican-2 (cerebroglycan) were detected in young cultures, but their expression decreased substantially as the neurons matured (Fig. 4 A). Only syndecan-2 and syndecan-4 showed temporal expression patterns consistent with the immunostaining results (Fig. 4 B). No syndecan-2 mRNA was detected at any time between plating and 8 DIV. Expression of syndecan-2 was first detectable at 9 DIV and then steadily increased to reach a plateau at 21 DIV, while syndecan-4 expression increased more abruptly at 30 DIV.

Syndecan-2 Localization in Dendritic Spines

To determine which syndecan is responsible for the spine-specific accumulation of heparan sulfate, hippocampal neurons at 30 DIV were stained with pAbs to syndecan-2 and syndecan-4 (Kim et al., 1994). This analysis revealed that syndecan-4 is not expressed in neurons, but in astrocytes which were present as a minor population in older cultures (data not shown). On the other hand, syndecan-2 is expressed in neurons in a time course and a pattern similar to those of heparan sulfate immunoreactivity. Syndecan-2 was localized on the surface of dendrites and cell bodies of hippocampal pyramidal neurons in a punctate pattern (Fig. 4, D–F). Syndecan-2 immunoreactivity was first detected at 2 wk in vitro. Then punctate staining became even stronger at 3 and 4 wk in vitro (Fig. 4, E and F). Double staining for synaptophysin, a presynaptic marker, and syndecan-2 showed partially overlapping patterns of staining, similar to the result of synapsin I/heparan sulfate double staining (see Fig. 2, A–C). Double staining with anti–syndecan-2 and anti–PSD-95 antibodies further confirmed a synaptic localization of syndecan-2 (Fig. 5, E–I). Punctate immunoreactivity for syndecan-2 and PSD-95 showed significant overlap mostly along dendrites (Fig. 5, E–G), although occasionally there were some PSD-95–positive dots that were not positive for syndecan-2 (see arrows in Fig. 5 G). These puncta are likely to represent

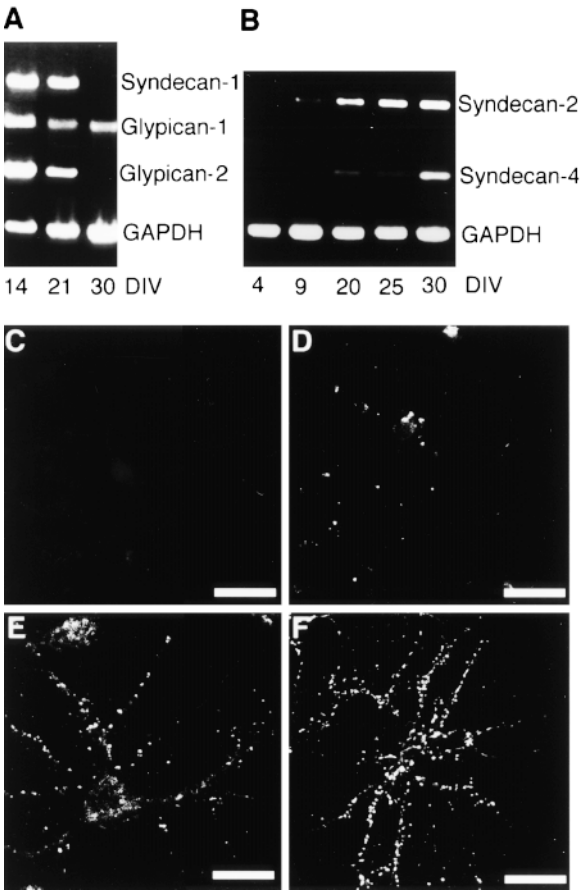

Figure 4. Time-dependent expression of different HSPGs in cultured hippocampal neurons. (A and B) RT-PCR analysis was performed with total RNA isolated from hippocampal neurons at indicated days in vitro. The amounts of total RNA were standardized by the expression level of glyceraldehyde 3-phosphate dehydrogenase (GAPDH). (A) RT-PCR analysis of syndecan-1, glypican-1, and glypican-3. (B) RT-PCR analysis of syndecan-2 and syndecan-4. Expression of syndecan-2 and syndecan-4 increases during the course of the culture. (C–F) Immunostaining of hippocampal neurons at 1 (C), 2 (D), 3 (E), and 4 (F) wk in culture with anti–syndecan-2 antibodies. Syndecan-2 immunoreactivity was first detected at 2 wk and then became stronger at 3 (E) and 4 (F) wk in vitro. Note that syndecan-2 was expressed in neurons in a time course and a pattern similar to that of the heparan sulfate immunostaining. Bar, 20 μm.

PSD-95 at nonsynaptic sites on dendritic shafts (Aoki, C., Z. Shusterman, M. Kasat, M. Bak, L. Alexandre, and D.S. Bredt. 1998. Society for Neuroscience Annual Meeting. Abstract 713.11). Together, these results strongly suggest that syndecan-2 is the cell surface HSPG predominantly localized on the dendritic spines of cultured hippocampal neurons. In adult rat brain, syndecan-2 has been shown recently to be highly concentrated at asymmetric synapses formed on the dendritic spines of pyramidal neurons in the CA3 area of the hippocampus (Hsueh et al., 1998). These observations further support our finding that syndecan-2 is one of the HSPGs responsible for the spine-specific accumulation of heparan sulfate on mature hippocampal neurons in vitro, though a contribution by unknown HSPGs has not been ruled out.

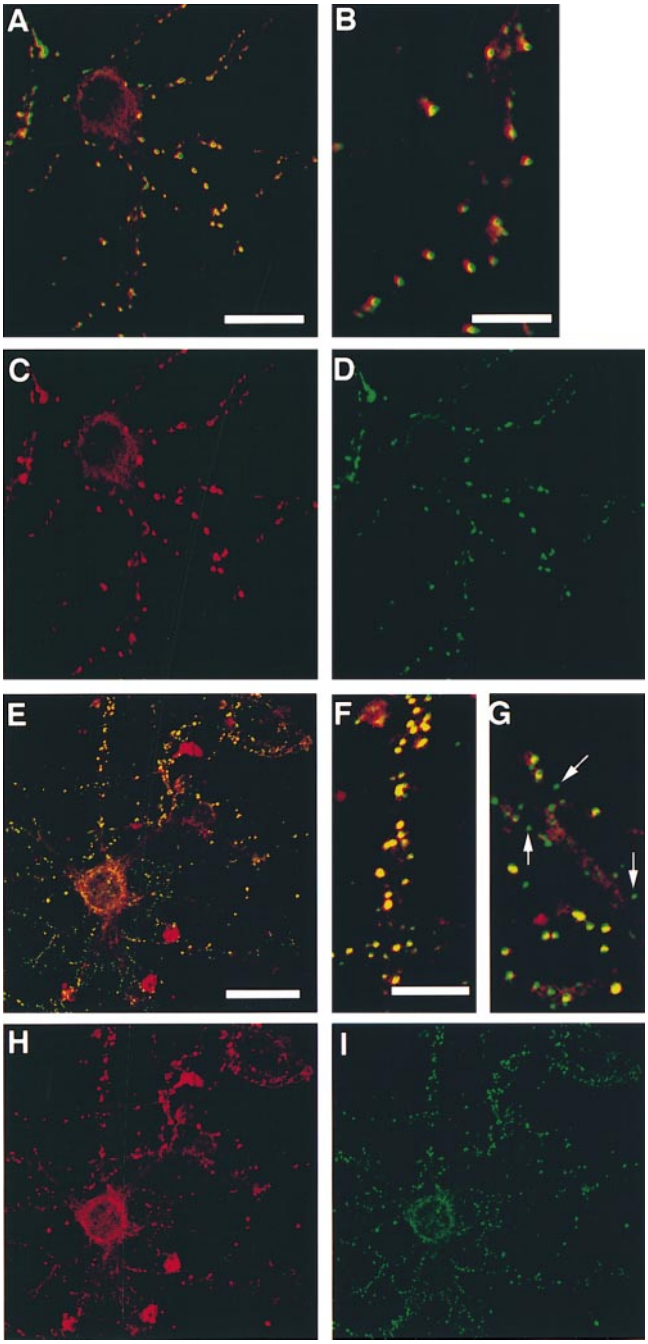

Figure 5. Postsynaptic localization of syndecan-2 on hippocampal neurons. (A–D) Double immunostaining of 30 DIV hippocampal neurons with antisynaptophysin (D, green) and anti–syndecan-2 (C, red) antibodies, and their overlap image (A and B). (B) High-power magnification of the boxed area in A. Immunoreactivities of synaptophysin and syndecan-2 show close apposition with partial overlap (yellow) as seen in the synapsin I/heparan sulfate double staining (see Fig. 2, A–E). Bars, 20 μm in A–C and 10 μm in D. (E–I) Double immunostaining with syndecan-2 (H, red) and PSD-95 (I, green) antibodies further confirmed synaptic localization of syndecan-2. (E–G) Punctate immunoreactivity for syndecan-2 was overlapping with PSD-95 immunolabeling mostly along dendrite (see yellow), although occasionally there were some PSD-95–positive dots (green) that are not positive for syndecan-2 (arrows in G), that may represent PSD-95 immunoreactivity at nonsynaptic sites on dendritic shaft (see Results). Bars, 20 μm in E and 7 μm in F.

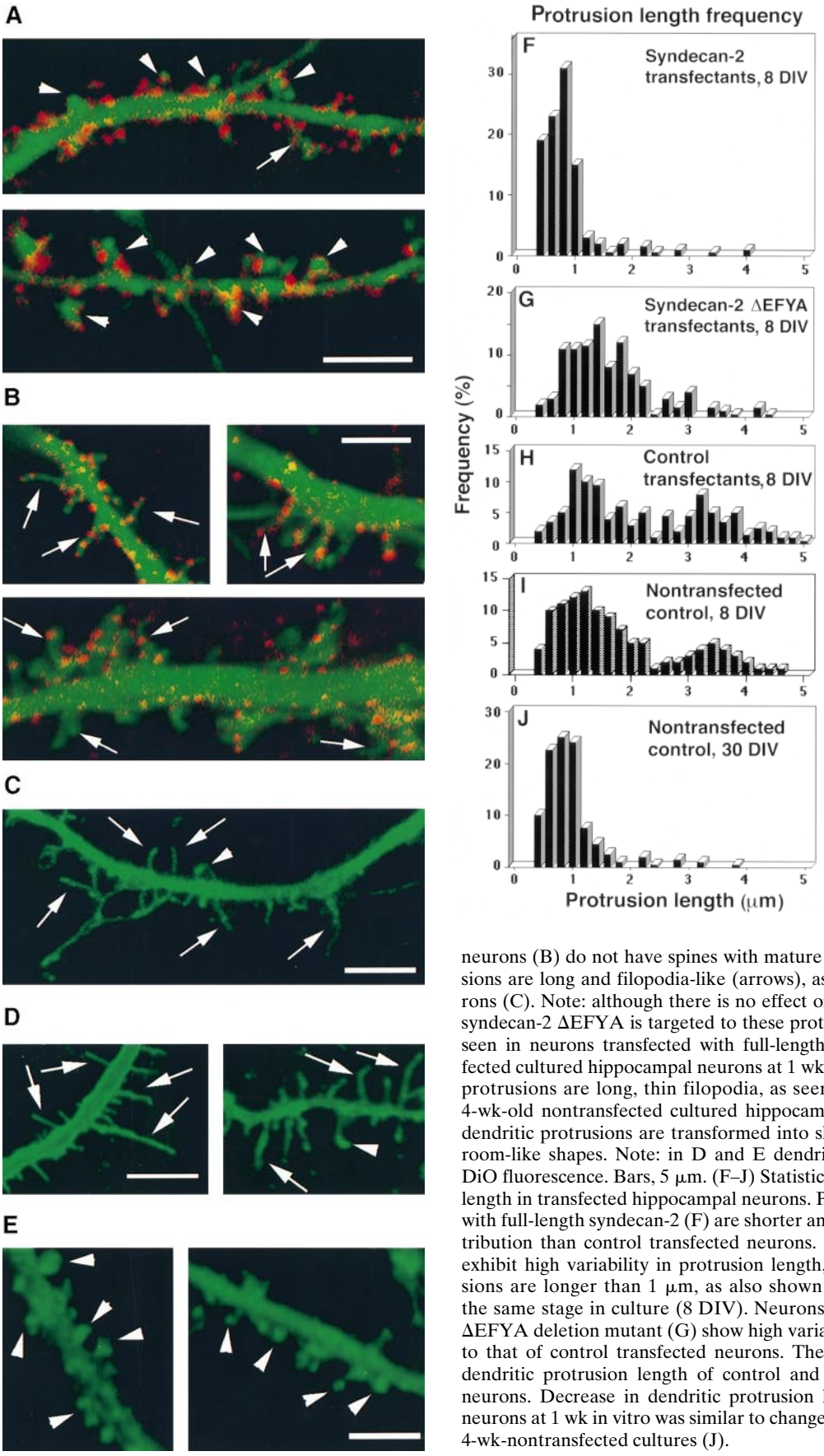

Figure 6. Forced expression of syndecan-2 in young hippocampal neurons induces the morphological maturation of dendritic spines. Hippocampal neurons at 1 DIV were cotransfected in 1:1 ratio with full-length syndecan-2 plus GFP (A) or with the syndecan-2 ΔEFYA deletion mutant plus GFP (B). Cells were analyzed 7 d after transfection by confocal microscopy after immunostaining with anti–syndecan-2 antibodies which recognize the extracellular domain of syndecan-2 (red). Those neurons that showed only GFP fluorescence, but were negative for syndecan-2, were considered as control transfected neurons (C). Note that the protrusions on neurons transfected with full-length syndecan-2 (A) are short and exhibit a mature spine morphology. Transfected syndecan-2 is expressed on these spines. Arrowheads indicate stubby and mushroom-shaped spines. In contrast, syndecan-2 ΔEFYA-transfected neurons (B) do not have spines with mature morphology. Most of the protrusions are long and filopodia-like (arrows), as seen in control transfected neurons (C). Note: although there is no effect on the morphology of protrusions, syndecan-2 ΔEFYA is targeted to these protrusions and forms clusters (B), as seen in neurons transfected with full-length syndecan-2 (A). (D) Nontransfected cultured hippocampal neurons at 1 wk in vitro, the majority of dendritic protrusions are long, thin filopodia, as seen in transfected control (C). (E) 4-wk-old nontransfected cultured hippocampal neurons. By 4 wk in culture dendritic protrusions are transformed into short spines with stubby or mushroom-like shapes. Note: in D and E dendritic protrusions are visualized by DiO fluorescence. Bars, 5 μm. (F–J) Statistical analysis of dendritic protrusion length in transfected hippocampal neurons. Protrusions in neurons transfected with full-length syndecan-2 (F) are shorter and exhibit more homogeneous distribution than control transfected neurons. Control transfected neurons (H) exhibit high variability in protrusion length, and the majority of the protrusions are longer than 1 μm, as also shown for untransfected control (I) at the same stage in culture (8 DIV). Neurons transfected with the syndecan-2 ΔEFYA deletion mutant (G) show high variability in protrusion length similar to that of control transfected neurons. There is no significant difference of dendritic protrusion length of control and syndecan-2 ΔEFYA transfected neurons. Decrease in dendritic protrusion length in syndecan-2 transfected neurons at 1 wk in vitro was similar to changes in dendritic protrusion length in 4-wk-nontransfected cultures (J).

Forced Expression of Syndecan-2 Induces Morphological Maturation of Dendritic Spines in Young Hippocampal Neurons

The highly specific localization of syndecan-2 on dendritic spines and the timing of its appearance suggest that syndecan-2 may be functionally involved in the development and maturation of dendritic spines. It has been shown that mature dendritic spines develop from thin, filopodia-like protrusions, and that this process is induced by the formation of contacts between the dendritic protrusions and nearby axons (Ziv and Smith, 1996). In cultured hippocampal neurons at 1 wk in vitro, the majority of dendritic protrusions are characterized as long, thin filopodia-like structures (Fig. 6 D; also see Papa et al., 1995; Ziv and Smith, 1996). During the next 2 wk, these filopodia-like protrusions actively initiate contacts with nearby axons, and by 3–4 wk in vitro, transform into mature spines with stubby or mushroom-like shapes (Fig. 6 E), as seen with hippocampal dendritic spines in vivo (Papa et al., 1995).

We hypothesized that, if syndecan-2 is functionally involved in spine development, then forced expression of syndecan-2 in young neurons would affect the morphology of spines. To test this hypothesis, hippocampal neurons were transfected at 1 DIV with syndecan-2 cDNA in an expression vector driven by the cytomegalovirus promoter. A GFP-expression vector was cotransfected with the syndecan-2 cDNA expression vector to visualize entire cell contours of transfected neurons, including dendritic protrusions. At 7 d after transfection (8 DIV), cultures cotransfected with syndecan-2 and GFP were examined for expression of exogenous syndecan-2 by immunostaining with anti–syndecan-2 antibodies and the morphology of dendritic protrusions by GFP fluorescence (see Fig. 4 C, endogenous syndecan-2 is not yet expressed at 8 DIV). Neurons transfected with GFP alone were considered as control transfected neurons.

We found remarkable morphological changes in the dendritic protrusions of syndecan-2 transfected neurons. While dendritic protrusions of control transfected neurons were highly variable in length (Fig. 6 H; control transfectants, 8 DIV), protrusions in syndecan-2 transfected neurons were shorter and more homogeneous in length (Fig. 6 F; syndecan-2 transfectants, 8 DIV; also see Table I). More remarkably, the majority of the protrusions in syndecan-2 transfected neurons had stubby or mushroom-like shapes with conspicuous heads (Fig. 6 A; arrowheads). Spines with these types of morphologies are typically found in mature neurons after 3 wk in vitro (Fig. 6, E and J; see also Papa et al., 1995), but are rarely observed in young neurons before 2 wk in vitro (Fig. 6 D and Table I). Immunofluorescent staining revealed that exogenous syndecan-2 was expressed as numerous dots along the dendrites, tightly associated with these spine-like structures (Figs. 6 A and 7 A). This pattern of distribution was similar to that of endogenous syndecan-2 after 3 wk in vitro (see Fig. 4, E and F). In contrast, dendritic protrusions of control transfected neurons showed no morphological changes. They showed thin, filopodia-like shapes (Fig. 6 C) as seen in normal nontransfected hippocampal neurons at the same stage in culture (Fig. 6 D).

To examine the specificity of the effect, we compared the morphological changes between syndecan-2–expressing and syndecan-2–nonexpressing cells in the same culture (Table I). When syndecan-2 and GFP expression vectors were cotransfected in a 1:1 ratio, ~30% of the GFP-positive neurons also expressed syndecan-2, while the others expressed GFP but not syndecan-2. These cells expressing only GFP served as an internal control for possible nonspecific effects of transfection. We found that neurons showing GFP fluorescence, but not syndecan-2 immunoreactivity, had dendritic protrusions with immature morphology similar to those seen in normal nontransfected neurons (Fig. 6, D and I), whereas neurons in the same culture that showed both GFP fluorescence and syndecan-2 immunoreactivity had spines with mature morphology (Table I). These results indicate that the effect of syndecan-2 transfection on spine morphology is not a nonspecific effect of transfection, but a specific effect of syndecan-2 expression.

Despite the changes in protrusion length and shape, the total number of dendritic protrusions was not altered by syndecan-2 transfection (12.2 ± 1.3 and 10.2 ± 1.6 protrusions per 50-μm segment of dendrite for syndecan-2 and control transfected neurons, respectively). Hence, these results indicate that the observed changes were due to morphological transformation of long filopodia into spines with mature morphologies, rather than the selective elimination of filopodia.

To examine whether these morphological changes in dendritic protrusions were accompanied by an increase in the number of synaptic contacts, we quantitated the number of synapsin I–positive presynaptic boutons in syndecan-2 transfected and control transfected neurons. Normally, the morphological changes from long, thin filopodia to mature spines occur after the formation of synaptic contacts with presynaptic axons. However, spine maturation induced by the early introduction of syndecan-2 into young neurons was not due to an acceleration of synaptogenesis. As shown in Table II, the number of synapsin I–positive presynaptic boutons did not increase in syndecan-2 transfected neurons. Moreover, only a portion of syndecan-2–positive protrusions with the mature spine-like morphology received presynaptic boutons (Table II).

Table I. Dendritic Protrusion Measurements

Time in culture	Proteins expressed	Protrusion's length	Protrusions with heads
		μm	*%*
8 DIV	Syndecan-2 and GFP	0.75–0.20*	75
8 DIV	Syndecan-2 ΔEFYA and GFP	1.57–0.47	21
8 DIV	GFP alone	1.52–0.50	28
8 DIV	None	1.67–0.51	18
30 DIV	None	0.85–0.20	71

Hippocampal neurons were transfected with full-length syndecan-2 and GFP or syndecan-2 ΔEFYA and GFP at 1:1 ratio as described in Materials and Methods. 7 d after transfection, neurons were stained with syndecan-2 antibody and examined under confocal microscope for the expression of exogenous syndecan-2 and the morphology of dendritic protrusions (by GFP fluorescence). Neurons expressing GFP but not syndecan-2 served as negative control for this experiment (GFP alone). Results represent the mean ± SD of the length of dendritic protrusions ($n \geq 200$).

*Significantly different from neurons expressing GFP alone, but not syndecan-2 (Student's *t* test). There is no significant difference of average dendritic protrusion length between GFP and syndecan-2 ΔEFYA expressing transfected neurons.

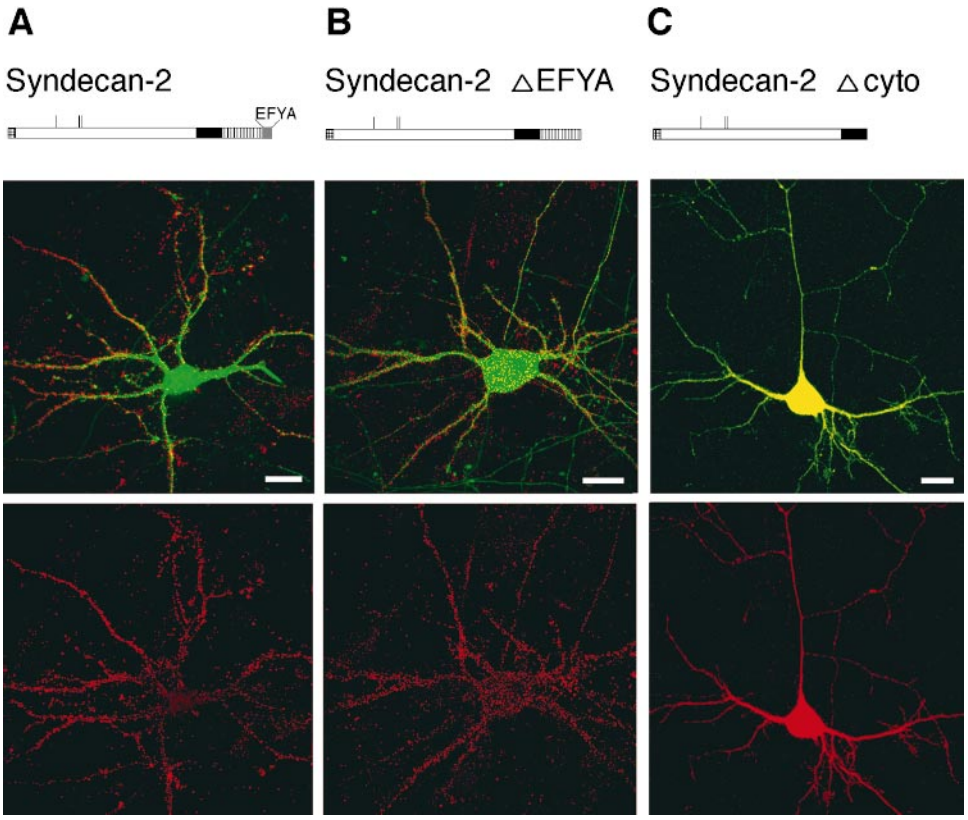

Figure 7. Cytoplasmic domain of syndecan-2, but not COOH-terminal PDZ binding motif, is required for the targeting of syndecan-2 to dendritic spines. Hippocampal neurons were transfected with full-length syndecan-2 (A), with the syndecan-2 ΔEFYA deletion mutant (B), or with the syndecan-2 Δcyto mutant (C). Neurons were cotransfected with GFP as in Fig. 6. Cells were analyzed 7 d after transfection by confocal microscopy after immunostaining with anti–syndecan-2 antibodies which recognize the extracellular domain of syndecan-2 (red). Both full-length syndecan-2 (A) and the syndecan-2 ΔEFYA deletion mutant (B) are sorted and expressed on dendritic spines/protrusions. In contrast, the syndecan-2 Δcyto deletion mutant does not show any specific sorting, being distributed diffusely on entire neuronal surfaces (C). Note: correct cell surface folding of syndecan-2 Δcyto deletion mutant was confirmed (see Results). Bars, 20 μm.

These results suggest that the early introduction of syndecan-2 into young neurons, before they establish synapses, circumvented this process and caused premature initiation of a spine maturation program.

Syndecan-2–induced Maturation of Dendritic Spines Requires the COOH-terminal EFYA Motif

Syndecan-2 has been shown recently to interact with at least two PDZ domain proteins, syntenin (Grootjans et al., 1997) and CASK (Cohen et al., 1998; Hsueh et al., 1998), through its COOH-terminal EFYA motif. The importance of PDZ domain proteins in synaptic organization has attracted increasing attention. The subsynaptic molecular lattice involving PSD-95 and CASK is thought to play a critical role in the organization of postsynaptic specialization by localizing signal transduction molecules and ligand-gated ion channels to the postsynaptic membrane (Naisbitt et al., 1997; reviewed in Craven and Bredt, 1998).

To investigate whether the syndecan-2–mediated maturation of dendritic spines involves the interaction of syndecan-2 with PDZ domain proteins, we transfected neurons with a syndecan-2 deletion mutant that lacked the COOH-terminal EFYA motif (syndecan-2 ΔEFYA). It has been shown that the EFYA motif is critical for binding to both syntenin and CASK (Grootjans et al., 1997; Cohen et al., 1998; Hsueh et al., 1998). We found that deletion of this PDZ domain binding motif abolished the ability of syndecan-2 to induce the morphological maturation of spines. In syndecan-2 ΔEFYA–transfected neurons, the majority of dendritic protrusions showed immature morphologies (Fig. 6 B) and were highly variable in length (Fig. 6 G, syndecan-2 ΔEFYA transfectants, 8 DIV), similar to those of control transfected neurons (Fig. 6, C and H, control transfected, 8 DIV). These results indicate that the effect of syndecan-2 on spine maturation requires the interaction of syndecan-2 with PDZ domain proteins expressed in hippocampal neurons.

Table II. Quantitative Analysis of the Effects of Syndecan-2/Syndecan-2 ΔEFYA Transfections on Synapse Formation and the Clustering of Syndecan-2

Transfection	Syndecan-2 (full-length)	Syndecan-2 ΔEFYA	GFP alone
Synapsin I–positive presynaptic boutons*	155.7 ± 20.8	135.8 ± 17.0	125.0 ± 20.3
Syndecan-2 clusters*	1,955 ± 235	1,882 ± 371	Not applicable

*Hippocampal neurons were transfected with full-length syndecan-2 and GFP or syndecan-2 ΔEFYA and GFP at a 10:1 ratio, or GFP alone as described in Materials and Methods. 7 d after transfection, neurons were stained with anti–synapsin I or anti–syndecan-2 antibodies. For each experiment, we analyzed 10 sampling windows (150 μm^2), each containing a single GFP-positive pyramidal neuron with its cell body and proximal dendrites, as seen in Fig. 7. The number of synapsin I–positive boutons and syndecan-2 clusters was digitally counted using MetaMorph software. Results represent the mean ± 1 SD (n = 10).

Targeting of Syndecan-2 to Dendritic Protrusions Requires the Cytoplasmic Domain But Not the EFYA Motif

Interestingly, although deletion of the PDZ domain bind-

ing motif abrogated the ability of syndecan-2 to induce spine maturation, it did not affect the targeting of syndecan-2 into dendritic protrusions. Syndecan-2 that lacked the EFYA motif was still sorted to dendrites and showed a punctate distribution (Fig. 7 B), similar to that of full-length syndecan-2 (Fig. 7 A). High-power views revealed the clustering of truncated syndecan-2 on dendritic protrusions that had immature morphologies (Fig. 6 B). In some instances, clusters of truncated syndecan-2 were found at the tips of the protrusions. Quantitative analysis showed that the numbers of syndecan-2 clusters in dendrites were essentially the same between full-length syndecan-2 and syndecan-2 ΔEFYA transfected neurons (Table II). However, clustering of syndecan-2 in dendritic protrusions was completely abolished in neurons transfected with another syndecan-2 mutant that lacked most of the cytoplasmic domain, except three juxtamembrane amino acids (syndecan-2 Δcyto). This three amino acid tail was left to ensure correct folding of the deletion mutant. A similar strategy was used by Carey et al. (1996) with a syndecan-1 deletion mutant that shares 100% homology with other syndecans in transmembrane and juxtamembrane cytoplasmic domains. Cell surface anchoring of our mutant was also confirmed by confocal microscopy in Z-plane (data not shown). Syndecan-2 Δcyto was diffusely distributed on the surface of neurons without any specific sorting pattern (Fig. 7 C). Together, these results demonstrate that the clustering of syndecan-2 on the dendritic protrusions is mediated, at least in part, by the cytoplasmic domain, but is independent of interactions with PDZ domain proteins, suggesting that a part of the cytoplasmic domain other than the EFYA motif is involved in the targeting of syndecan-2 to dendritic protrusions.

Discussion

In this paper, we present evidence that the cell surface heparan sulfate proteoglycan syndecan-2 plays a significant functional role in the structural transformation of dendritic protrusions into mature spines. We demonstrate that syndecan-2 is specifically localized on the dendritic spines of cultured hippocampal neurons, coinciding with the morphological maturation of the spines. Syndecan-2 introduced by transfection into young hippocampal neurons is targeted to dendritic protrusions, and induces their early morphological maturation into spine-like structures. The COOH-terminal EFYA motif of syndecan-2, the binding site for PDZ domain proteins, is required for the maturation-inducing effect of syndecan-2, but is not essential for the targeting of syndecan-2 to dendritic protrusions. These results suggest that molecular interactions involving syndecan-2 play a significant role in the organization of postsynaptic structures.

The interaction of syndecan-2 with PDZ domain proteins has been reported recently by different groups. Grootjans et al. (1997) identified a novel PDZ domain protein called syntenin by yeast two-hybrid screening, using the cytoplasmic domain of syndecan-2 as a bait. More recently, yeast two-hybrid screening identified the cytoplasmic domain of syndecan-2 as a ligand for CASK (Cohen et al., 1998; Hsueh et al., 1998). Hsueh et al. (1998) have further demonstrated that syndecan-2 is present in the vicinity of synapses in adult rat brain. By using cultures of rat hippocampal neurons, we have been able to localize syndecan-2 to the dendritic spines of mature hippocampal pyramidal neurons. Moreover, we showed that the accumulation of syndecan-2 on dendritic spines occurs concomitant with their structural maturation. These observations indicate that syndecan-2 is actively targeted to, and accumulated on, dendritic spines by a developmentally regulated mechanism.

The most intriguing finding of our study is that syndecan-2, when transfected into young neurons, directly influences the morphology of dendritic protrusions, transforming them into mature spine-like structures with characteristic shapes. This effect was clearly due to syndecan-2, as syndecan-2 deletion mutants did not show these changes. Transfected full-length syndecan-2 was indeed expressed on the dendritic protrusions that had undergone morphological reorganization. Abnormalities in dendritic spine development have been found in some forms of mental retardation and autism (Rudelli et al., 1985; Hinton et al., 1991; Comery et al., 1997). Interestingly, recent findings have shown that the syndecan-2 gene may be inactivated by positional effects in a patient with autism, mental retardation, and multiple exostoses (Ishikawa-Brush et al., 1997). It is tempting to speculate that the deficiency in dendritic spine maturation, seen in patients with these neurodevelopmental disorders, might be caused by misexpression of syndecan-2.

As to how syndecan-2 induces the formation of morphologically mature spines is now an important question in understanding the mechanism of spine development. Our results have provided some preliminary insight into this process. We found that the COOH-terminal EFYA motif of syndecan-2 is required for the induction of spine maturation by syndecan-2. These results strongly suggest that interaction with PDZ domain proteins is essential for this effect. CASK, which has been shown to be expressed in synapses, is the most likely candidate for the syndecan-2 ligand in spines, although other PDZ domain proteins may also be involved.

While syndecan-2 is specifically localized in the synaptic junctions of mature neurons, CASK is not exclusively concentrated at synapses, but is also present in a variety of membrane compartments in neurons, and its compartmentalization between membrane and cytoplasm may be regulated by an as yet unknown mechanism (Hsueh et al., 1998). Our transfection experiments with syndecan-2 lacking the EFYA motif (syndecan-2 ΔEFYA) illuminates a new view on this matter. While the EFYA motif (PDZ domain binding site) is required for the morphological maturation of spines in syndecan-2 transfected neurons, a mutant lacking the EFYA motif still clustered in dendritic protrusions. Therefore, clustering of syndecan-2 in spines occurs independent of (or before) its interaction with PDZ domain proteins. However, deletion of the cytoplasmic domain of syndecan-2 abolished its clustering in dendritic protrusions. This finding indicates that a region of the cytoplasmic domain, excluding the EFYA motif, is necessary for this process. Thus, it appears more likely that syndecan-2 first clusters on dendritic membranes and then recruits CASK and/or other PDZ domain proteins to membrane compartments within the vicinity of synapses.

The cytoplasmic domain of syndecan-2 contains four potential tyrosine phosphorylation sites shared by all syndecans (Asundi and Carey, 1997), and unique serine phosphorylation sites that can be phosphorylated by Ca^{2+}-dependent and conventional isoforms of PKC α, β and γ (Oh et al., 1997). It is conceivable that phosphorylation of some of these residues is involved in the clustering of syndecan-2 on the spines. A role for PKC in synaptic plasticity and memory storage has been proposed (Wang and Feng, 1992; Klann et al., 1993; Van der Zee and Douma, 1997; Zeeuw et al., 1998). It has been shown that the postsynaptic substrates for PKC activity, RC3/neurogranin and adducin, are targeted to dendritic spines and are involved in their development (Neuner-Jehle et al., 1996; reviewed in Gerendasy and Sutcliffe, 1997; Matsuoka et al., 1998). Matsuoka et al. (1998) have suggested that external signals cause the PKC-dependent phosphorylation of adducin in dendritic spines that results in reorganization of cytoskeletal structures and morphological changes of spines. Thus it is possible that the phosphorylation of syndecan-2 by PKC may also be involved in its sorting and clustering on dendritic spines in response to extracellular ligands, such as components of the extracellular matrix or growth factors.

It is interesting to note that extracellular interactions are essential for the clustering of syndecan-1 on the cell surface (Carey et al., 1994). In this vein, we found that the number of syndecan-2 clusters that appeared on dendrites of syndecan-2 transfected neurons correlates well with the cell density of transfected neurons. When the cell density was reduced to 25 and 50% of the regular plating condition (from 200,000 cells per 12-mm coverslip to 50,000 and 100,000 cells per coverslip), the number of syndecan-2 clusters decreased to 28 ± 8% and 54 ± 10%, respectively. As the frequency of axo-dendritic contacts is thought to increase in parallel with the cell density in the culture, this observation suggests that the formation of syndecan-2 clusters may be contact dependent. Thus it is tempting to speculate that the targeting and clustering of syndecan-2 may be triggered by extracellular ligands for syndecan-2. Such putative ligands may be presented by axons making contact with dendrites and those extracellular interactions work in conjunction with cytoplasmic phosphorylation to localize syndecan-2 to dendritic spines.

Further studies will be required to fully understand the roles of phosphorylation and the putative extracellular ligand(s) in the process of syndecan-2–induced spine maturation. Nevertheless, the current knowledge suggests the following scenario. Upon the initiating signal, which might be provided by the contact between dendritic protrusions, and axons, syndecan-2 is translocated to immature dendritic protrusions, and forms clusters by a mechanism that probably involves the phosphorylation of its cytoplasmic domain. Clustered syndecan-2 then recruits CASK and/or other PDZ domain proteins to dendritic protrusions. The recruitment of PDZ domain proteins to the inner surface of dendritic membranes would lead to the organization of cytoskeletal and signaling molecules at these sites, resulting in the formation of mature dendritic spines.

We have shown here the first evidence that a cell surface HSPG can cause structural modifications to dendritic spines. Our results suggest that molecular interactions involving syndecan-2 play a critical role in the organization of postsynaptic structures. Elucidation of the molecular mechanism by which syndecan-2 modifies postsynaptic sites will provide insight into the functional relationship between cell surface adhesion events and intracellular cytoskeletal signaling complexes in the regulation of synaptic plasticity.

We thank Drs. Merton Bernfield, Andrew Czernik, and Vladimir Berezin for their gifts of antibodies, Drs. W. Stallcup, B. Ranscht, and D. Ethell for helpful discussion and critical reading of the manuscript, and Dr. E. Monosov for his advice on confocal imaging.

This work was supported by National Institutes of Health grants HD25938 and NS33117.

Received for publication 20 October 1998 and in revised form 24 December 1998.

References

Asundi, V.K., and D.J. Carey. 1997. Phosphorylation of recombinant N-syndecan (syndecan-3) core protein. *Biochem. Biophys. Res. Commun.* 240:502–506.

Bernfield, M., R. Kokenyesi, M. Kato, M.T. Hinkes, J. Spring, R.L. Gallo, and E.J. Lose. 1992. Biology of the syndecans: a family of transmembrane heparan sulfate proteoglycans. *Annu. Rev. Cell Biol.* 8:365–393.

Brewer, G.J., and C.W. Cotman. 1989. Survival and growth of hippocampal neurons in defined medium at low density: advantage of a sandwich culture technique or low oxygen. *Brain Res.* 494:65–74.

Buchs, P.-A., and D. Muller. 1996. Induction of long-term potentiation is associated with major ultrastructural changes of activated synapses. *Proc. Natl. Acad. Sci. USA.* 93:8040–8045.

Calverley, R.K.S., and D.G. Jones. 1990. Contributions of dendritic spines and perforated synapses to synaptic plasticity. *Brain Res. Rev.* 15:215–249.

Carey, D.J. 1997. Syndecans: multifunctional cell-surface co-receptors. *Biochem. J.* 327:1–16.

Carey, D.J., R.C. Stahl, B. Tucker, K.A. Bendt, and G. Cizmeci-Smith. 1994. Aggregation-induced association of syndecan-1 with microfilaments mediated by the cytoplasmic domain. *Exp. Cell Res.* 214:12–21.

Carey, D.J., K.M. Bendt, and R.C. Stahl. 1996. The cytoplasmic domain of syndecan-1 is required for cytoskeleton association but not detergent insolubility. Identification of essential cytoplasmic domain residues. *J. Biol. Chem.* 271:15253–15260.

Chen, C., and H. Okayama. 1987. High-efficiency transformation of mammalian cells by plasmid DNA. *Mol. Cell. Biol.* 7:2745–2752.

Cohen, A.R., D.F. Wood, S.M. Marfatia, Z. Walther, A.H. Chishti, and J.M. Anderson. 1998. Human CASK/LIN-2 binds syndecan-2 and protein 4.1 and localizes to the basolateral membrane of epithelial cells. *J. Cell Biol.* 142: 129–138.

Cole, G.J., and W. Halfter. 1996. Agrin: an extracellular matrix heparan sulfate proteoglycan involved in cell interactions and synaptogenesis. *Perspect. Dev. Neurobiol.* 3:359–371.

Colman, D.R. 1997. Neurites, synapses, and cadherins reconciled. *Mol. Cell. Neurosci.* 10:1–6.

Comery, T.A., C.X. Stamoudis, S.A. Irwin, and W.T. Greenough. 1996. Increased density of multiple-head dendritic spines on medium-sized spiny neurons of the striatum in rats reared in a complex environment. *Neurobiol. Learn. Mem.* 66:93–96.

Comery, T.A., J.B. Harris, P.J. Willems, B.A. Oostra, S.A. Irwin, I.J. Weiler, and W.T. Greenough. 1997. Abnormal dendritic spines in fragile X knockout mice: maturation and pruning deficits. *Proc. Natl. Acad. Sci. USA.* 94:5401–5404.

Couchman, J.R., and A. Woods. 1996. Syndecans, signaling and cell adhesion. *J. Cell. Biochem.* 61:578–584.

Craven, S.E., and D.S. Bredt. 1998. PDZ proteins organize synaptic signaling pathways. *Cell.* 93:495–498.

David, G., X.M. Bai, B. Van der Schueren, J.J. Cassiman, and H. Van der Berghe. 1992. Developmental changes in heparan sulfate expression: in situ detection with mAbs. *J. Cell Biol.* 119:961–975.

David, G., X.M. Bai, B. Van der Schueren, P. Marynen, J.-J. Cassiman, and H. Van der Berghe. 1993. Spatial and temporal changes in the expression of fibroglycan syndecan-2 during mouse embryonic development. *Development.* 119:841–854.

Durand, G.M., Y. Kovalchuk, and A. Konnerth. 1996. Long-term potentiation and functional synapse induction in developing hippocampus. *Nature.* 381: 71–75.

Edwards, F.A. 1995. LTP: a structural model to explain the inconsistencies. *Trends Neurosci.* 18:250–255.

Eldridge, C.F., J.R. Sanes, A.Y. Chiu, R.P. Bunge, and C.J. Cornbrooks. 1986. Basal lamina-associated heparan sulphate proteoglycan in the rat PNS: characterization and localization using monoclonal antibodies. *J. Neurocytol.* 15: 37–51.

Fifkova, E. 1985. A possible mechanism of morphometric changes in dendritic

spines induced by stimulation. *Cell. Mol. Neurobiol.* 5:47–63.
Fuxe, K., B. Tinner, W. Staines, G. David, and L.F. Agnati. 1997. Regional distribution of neural cell adhesion immunoreactivity in the adult rat telencephalon and diencephalon. Partial colocalization with heparan sulfate proteoglycan immunoreactivity. *Brain Res.* 746:25–33.
Gerendasy, D.D., and J.G. Sutcliffe. 1997. RC3/neurogranin, a postsynaptic calpacitin for setting the response threshold to calcium influxes. *Mol. Neurobiol.* 15:131–163.
Goedert, M., R. Jakes, M.G. Spillantini, M. Hasegawa, M.J. Smith, and R.A. Crowther. 1996. Assembly of microtubule-associated protein tau into Alzheimer-like filaments induced by sulfated glycosaminoglycans. *Nature.* 383: 550–553.
Grootjans, J.J., P. Zimmermann, G. Reekmans, A. Smets, G. Degeest, J. Durr, and G. David. 1997. Syntenin, a PDZ protein that binds syndecan cytoplasmic domains. *Proc. Natl. Acad. Sci. USA.* 94:13683–13688.
Hagler, D.J., Jr., and Y. Goda. 1998. Synaptic adhesion: the building blocks of memory? *Neuron.* 20:1059–1062.
Harris, K.M., and S.B. Kater. 1994. Dendritic spines: cellular specializations imparting both stability and flexibility to synaptic function. *Annu. Rev. Neurosci.* 17:341–371.
Hebb, D.O. 1949. The Organization of Behavior. John Wiley & Sons Inc., New York. 335 pp.
Hinton, V.J., W.T. Brown, K. Wisniewski, and R.D. Rudelli. 1991. Analysis of neocortex in three males with the fragile X syndrome. *Am. J. Med. Genet.* 41: 289–294.
Hsueh, Y.P., F.C. Yang, V. Kharazia, S. Naisbitt, A.R. Cohen, R.J. Weinberg, and M. Sheng. 1998. Direct interaction of CASK/LIN-2 and syndecan heparan sulfate proteoglycan and their overlapping distribution in neuronal synapses. *J. Cell Biol.* 142:139–151.
Ishikawa-Brush, Y., J.F. Powell, P. Bolton, A.P. Miller, F. Francis, H.F. Willard, H. Lehrach, and A.P. Monaco. 1997. Autism and multiple exostoses associated with an X;8 translocation occurring within the GRPR gene and 3′ to the SDC2 gene. *Hum. Mol. Genet.* 6:1241–1250.
Itano, N., K. Oguri, Y. Nagayasu, Y. Kusano, H. Nakanishi, G. David, and M. Okayama. 1996. Phosphorylation of a membrane-intercalated proteoglycan, syndecan-2 expressed in stroma-inducing clone from a mouse Lewis lung carcinoma. *Biochem. J.* 315:925–930.
Kim, C.W., O.A. Goldberger, R.L. Gallo, and M. Bernfield. 1994. Members of the syndecan family of heparan sulfate proteoglycans are expressed in distinct cell-, tissue-, and development-specific patterns. *Mol. Biol. Cell.* 5:797–805.
Klann, E., S.-J. Chen, and J.D. Sweatt. 1993. Mechanism of protein kinase C activation during the induction and maintenance of long-term potentiation probed using a selective peptide substrate. *Proc. Natl. Acad. Sci. USA.* 90: 8337–8341.
Kornau, H.-C., L.T. Schenker, M.B. Kennedy, and P.H. Seeburg. 1995. Domain interaction between NMDA receptor subunits and the postsynaptic density protein PSD-95. *Science.* 269:1737–1740.
Lund, J.S., S.M. Holbach, and W.W. Chung. 1991. Postnatal development of thalamic recipient neurons in the monkey striate cortex. II. Influence of afferent driving on spine acquisition and dendritic growth of layer 4C spiny stellate neurons. *J. Comp. Neurol.* 309:129–140.
Lüthi, A., J.P. Laurent, A. Figurov, D. Muller, and M. Schachner. 1994. Hippocampal long-term potentiation and neural cell adhesion molecules L1 and NCAM. *Nature.* 372:777–779.
Matsuoka, Y., X. Li, and V. Bennett. 1998. Adducin is an in vitro substrate for protein kinase C: phosphorylation in the MARCKS-related domain inhibits activity in promoting spectrin-actin complexes and occurs in many cells, including dendritic spines of neurons. *J. Cell Biol.* 142:485–497.
Meier, T., F. Masciulli, C. Moore, F. Schoumacher, U. Eppenberger, A.J. Denzer, G. Jones, and H.R. Brenner. 1998. Agrin can mediate acetylcholine receptor gene expression in muscle by aggregation of muscle-derived neuregulins. *J. Cell Biol.* 141:715–726.
Milner, B., L.R. Squire, and E.R. Kandel. 1998. Cognitive neuroscience and the study of memory. *Neuron.* 20:445–468.
Naisbitt, S., E. Kim, R.J. Weinberg, A. Rao, F.C. Yang, A.M. Craig, and M. Sheng. 1997. Characterization of guanylate kinase-associated protein, a postsynaptic density protein at excitatory synapses that interacts directly with postsynaptic density-95/synapse-associated protein 90. *J. Neurosci.* 17: 5687–5696.
Neuner-Jehle, M., J.P. Denizot, and J. Mallet. 1996. Neurogranin is locally concentrated in rat cortical and hippocampal neurons. *Brain Res.* 733:149–154.
Oh, E.-S., J.R. Couchman, and A. Woods. 1997. Serine phosphorylation of syndecan-2 proteoglycan cytoplasmic domain. *Arch. Biochem. Biophys.* 344:67–74.
Papa, M., M.C. Bundman, V. Greenberger, and M. Segal. 1995. Morphological analysis of dendritic spine development in primary cultures of hippocampal neurons. *J. Neurosci.* 15:1–11.
Rollenhagen, A., and H.J. Bischof. 1994. Spine morphology of neurons in the avian forebrain is affected by rearing conditions. *Behav. Neural. Biol.* 62:83–89.
Rose, S.P.R. 1995. Cell-adhesion molecules, glucocorticoids and long-term-memory formation. *Trends Neurosci.* 18:502–506.
Rudelli, R.D., W.T. Brown, K. Wisniewski, E.C. Jenkins, M. Laure-Kamionowska, F. Connell, and H.M. Wisniewski. 1985. Adult fragile X syndrome. Clinico-neuropathologic findings. *Acta Neuropathol.* 67:289–295.
Schubert, D. 1991. The possible role of adhesion in synaptic modification. *Trends Neurosci.* 14:127–130.
Serafini, T. 1997. An old friend in a new home: cadherins at the synapse. *Trends Neurosci.* 20:322–323.
Spacek, J., and K.M. Harris. 1998. Three-dimensional organization of cell adhesion junctions at synapses and dendritic spines in area CA1 of the rat hippocampus. *J. Comp. Neurol.* 393:58–68.
Van der Zee, E.A., and B.R. Douma. 1997. Historical review of research on protein kinase in learning and memory. *Prog. Neuro-psychopharmacol. Biol. Psychiatry.* 21:379–406.
Wallace, C.S., N. Hawrylak, and W.T. Greenough. 1991. Studies of synaptic structural modifications after long-term potentiation and kindling: context for a molecular morphology. *In* Long-Term Potentiation: A Debate of Current Issues. M. Baudry and J.L. Davis, editors. MIT Press, Cambridge, MA. 189–232.
Wang, J.-H., and D.-P. Feng. 1992. Postsynaptic protein kinase C essential to induction and maintenance of long-term potentiation in the hippocampal CA1 region. *Proc. Natl. Acad. Sci. USA.* 89:2576–2580.
Watanabe, K., and Y. Yamaguchi. 1996. Molecular identification of a putative human hyaluronan synthase. *J. Biol. Chem.* 271:22945–22948.
Woods, A., and J.R. Couchman. 1994. Syndecan-4 heparan sulfate proteoglycan is a selectively enriched and widespread focal adhesion component. *Mol. Biol. Cell.* 5:183–192.
Yuste, R., and W. Denk. 1995. Dendritic spines as basic functional units of neuronal integration. *Nature.* 375:682–684.
Zafra, F., B. Hengerer, J. Leibrock, H. Thoenen, and D. Lindholm. 1990. Activity dependent regulation of BDNF and NGF mRNAs in the rat hippocampus is mediated by non-NMDA glutamate receptors. *EMBO (Eur. Mol. Biol. Organ.) J.* 9:3545–3550.
Zeeuw, D.C.I., C. Hansel, F. Bian, S.K.E. Koekkoek, A.M. van Alphen, D.J. Linden, and J. Oberdick. 1998. Expression of a protein kinase C inhibitor in Purkinje cells blocks cerebellar LTD and adaptation of the vestibulo-ocular reflex. *Neuron.* 20:495–508.
Ziv, N.E., and S.J. Smith. 1996. Evidence for a role of dendritic filopodia in synaptogenesis and spine formation. *Neuron.* 17:91–102.